Southern University of Science and Technology

Nonlinear coupling among turbulence, GAM and tearing modes in the edge of HL-2A plasmas

Jingchun Li

2022.9.27

Self-introduction

Name： Jingchun LI

Age： 32

Birthplace: Hunan, China

Major： Nuclear fusion and plasma physics

Phone： 18801109042

E-mail： jingchunli@pku.edu.cn

Research interest:

Micro-instabilities & turbulence, MHD instabilities, Gyro-kinetic simulation, High performance computing, Data analysis, etc

SUSTech Southern University of Science and Technology

目录

CATALOGUE

Background

- Multiscale interactions.
  - Multi-scale interactions between large-scale magnetohydrodynamic (MHD) instabilities and microscale turbulence is a crucial topic in magnetically confined plasma research;
  - Usually, when the turbulence flow is saturated, there will be mesoscale zonal flow, which forms a negative feedback system with the turbulence;
  - Drift waves may generate seed magnetic islands and develop into NTMs;

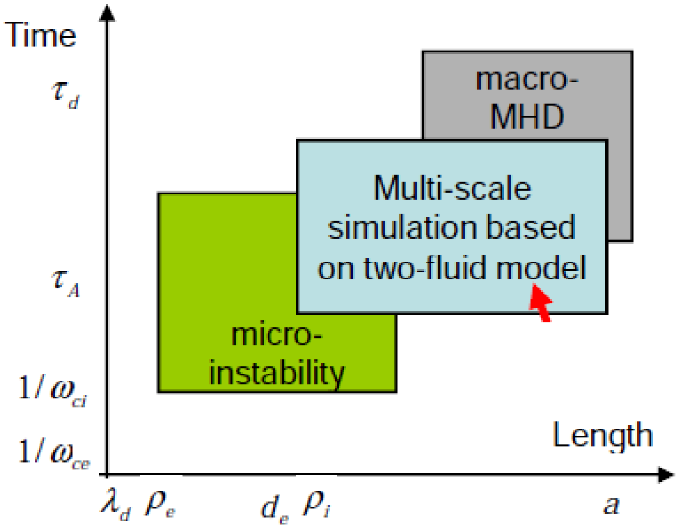

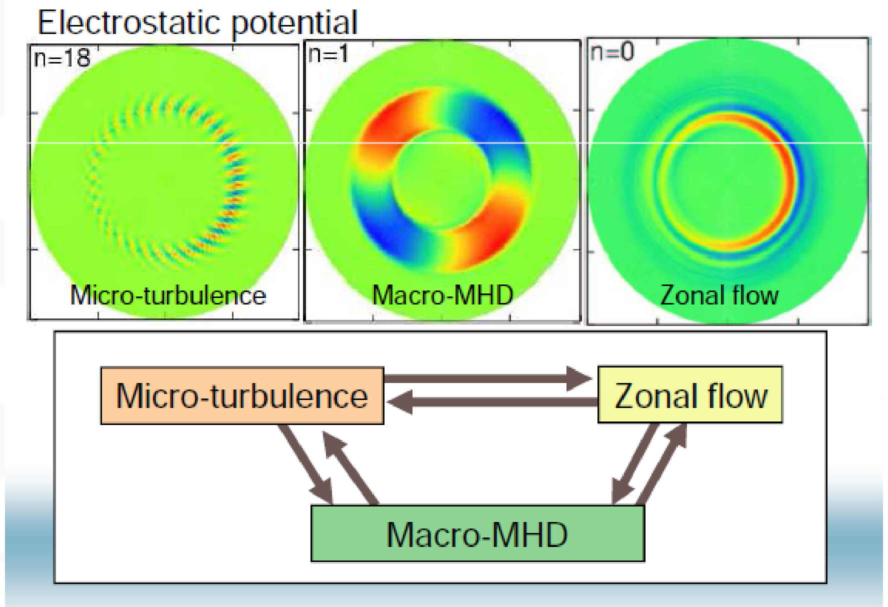

P.H. Diamond et.al., Phys. Fluids, (1984), S.-I. Itoh et. al., Phys. Rev. Lett., (2003)
M. Yagi, et al., Nuclear Fusion, (2005), A. Ishizawa, Phys. Plasmas (2007)
L. Bardóczi et al Phys. Rev. Lett. (2021), M.J. Choi et al Nature Comm. (2021)

Background

SUSTech Southern University of Science and Technology

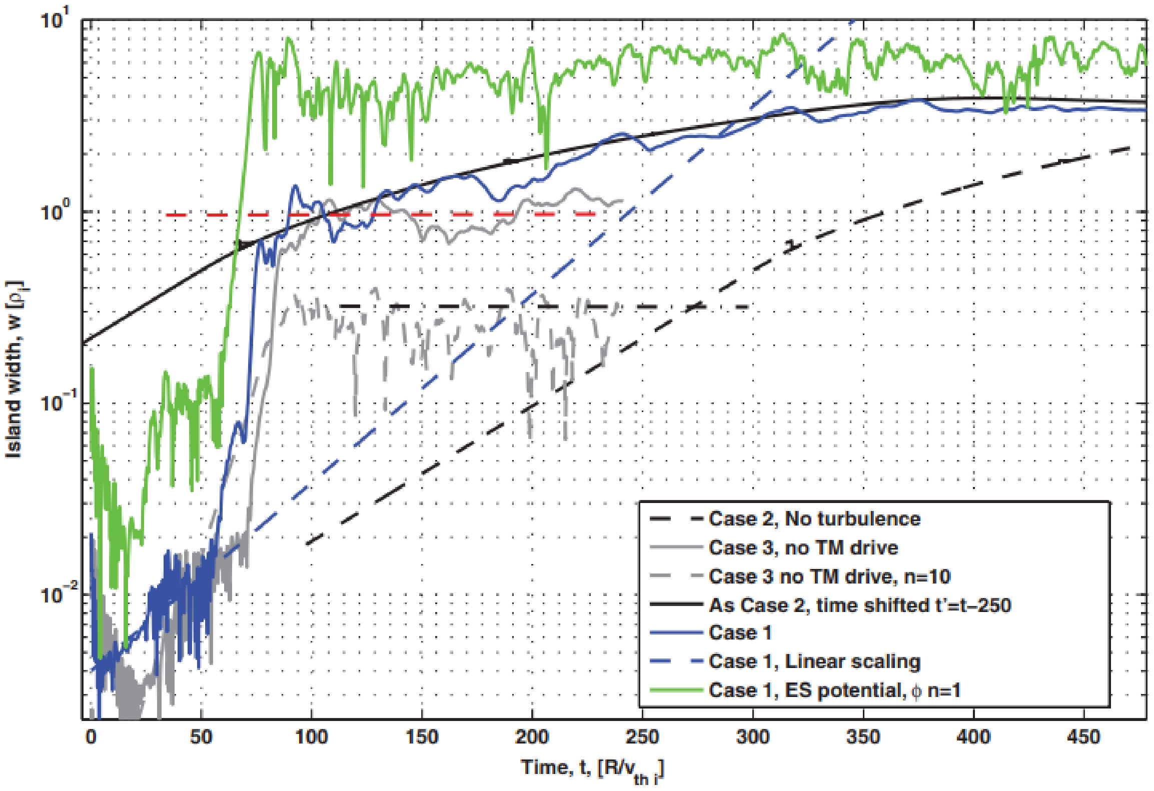

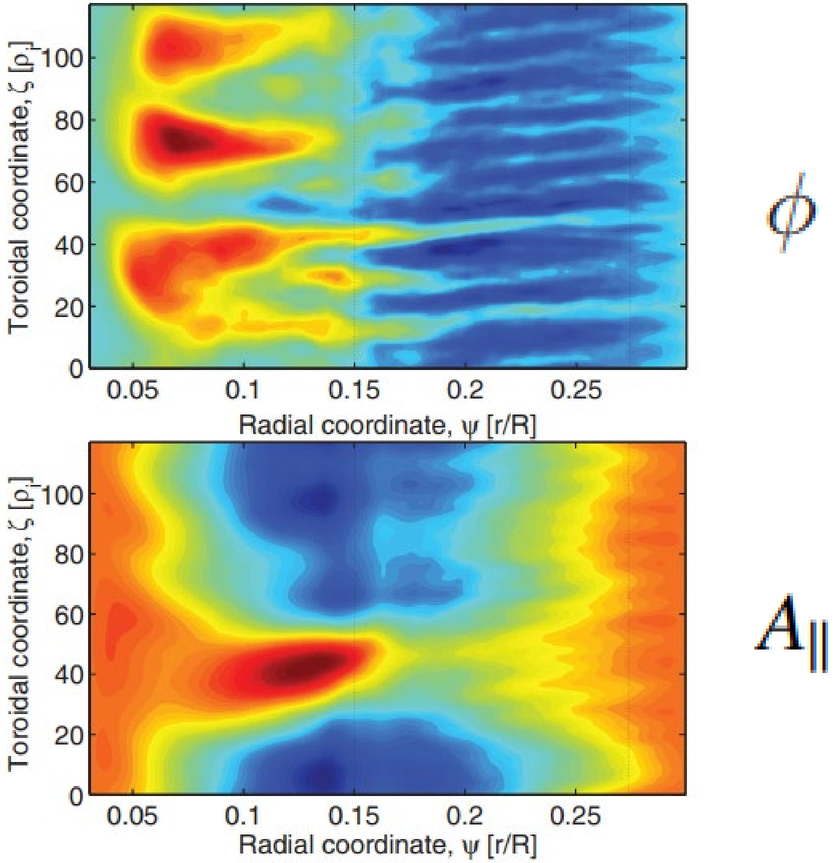

W A Hornsby et al PPCF 58 (2016) 014028

- The turbulence driven magnetic island (TDMI) has been discovered in fluid simulations, where it is shown the MI is formed due to a nonlinear beating of the fastest growing small scale modes [Muraglia M. 2011 PRL]
- Gyrokinetic simulations have also demonstrated that the electromagnetic turbulence is able to seed the magnetic island **(MI)** whose nonlinear evolution depends on the **plasma beta** and equilibrium **pressure gradient**.

SUSTech Southern University of Science and Technology

ITG turbulence stabilized by MI

P. Jiang, Z. Lin et al. 2014;
Bañón Navarro et al. 2017

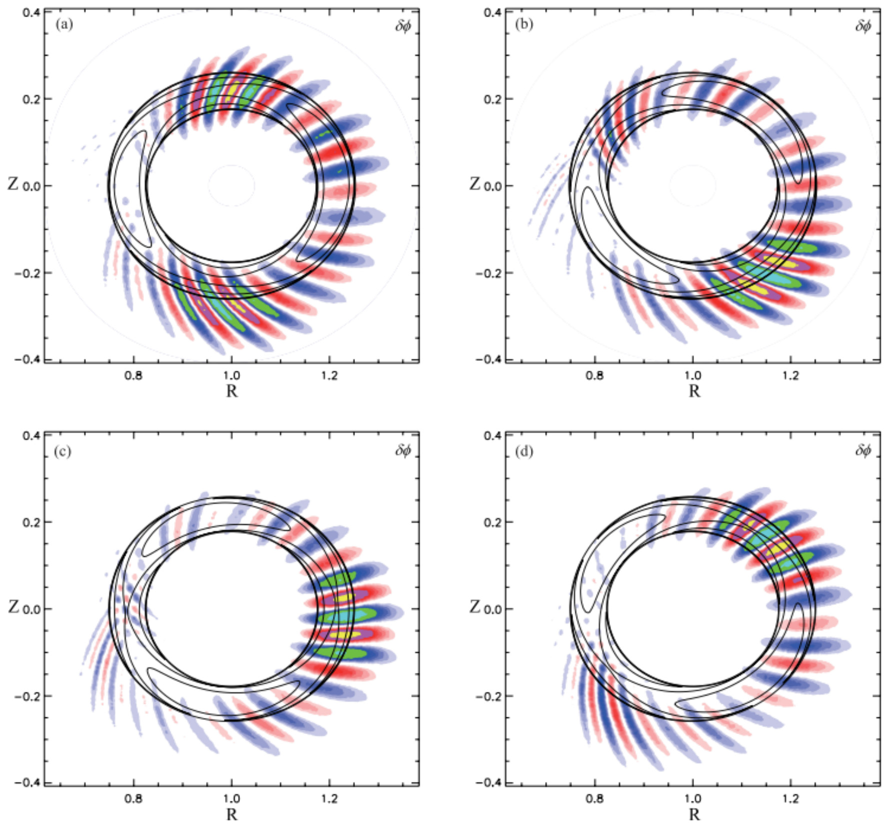

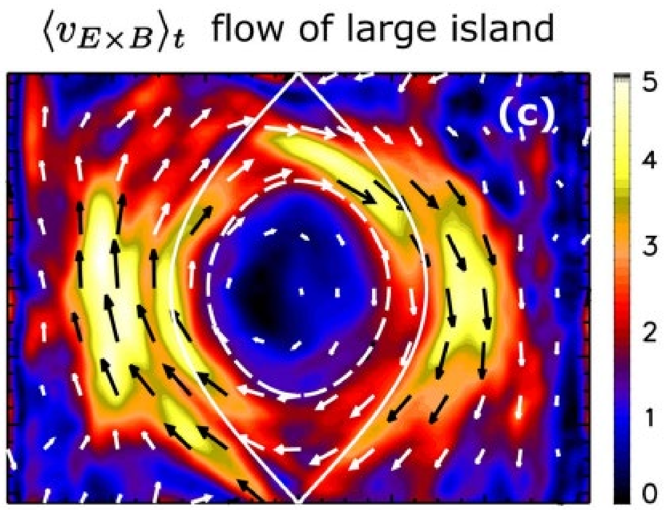

- The linear mode structures are **enhanced** at the island separatrices and **weakened** at the island centers, consistent with the flattening of the pressure profile inside the islands.
- E×B flow shearing is produced, this asymmetric shear **reduces** turbulence penetration into the island on the side where the shear is increased. This shows that shear flows sustain the low level of the turbulence in MI.

Nonlinear coupling induced by MI

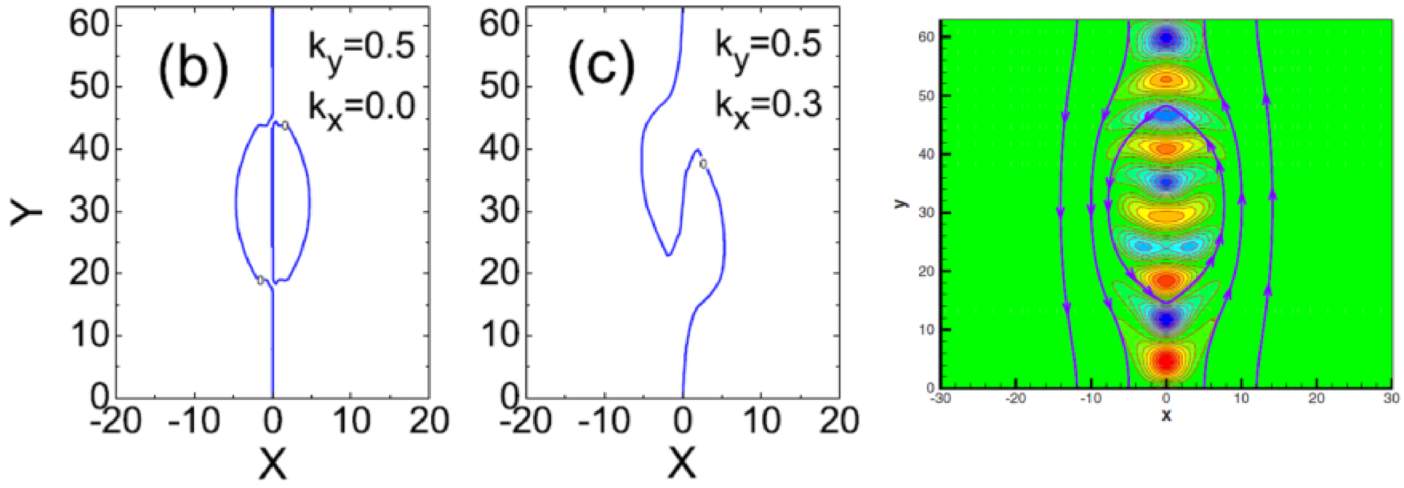

Z X Wang et al Phys. Plasmas 16, 060703 (2009)

- Using a gyrofluid model, Wang et al shows that when the magnetic island is wide enough to produce a **broad distribution** of rational surfaces near the O-point region, the ITG perturbations at these rational surfaces form a radially **global-type** eigenmode with a fast growth rate, which is referred to as the magnetic-island-induced ITG mode(MITG).
- When there is a MI, the RS is not a staightline, it has a profile in the the radial direction. (form a global ITG in MI)

SUSTech Southern University of Science and Technology

Nonlinear coupling induced by MI

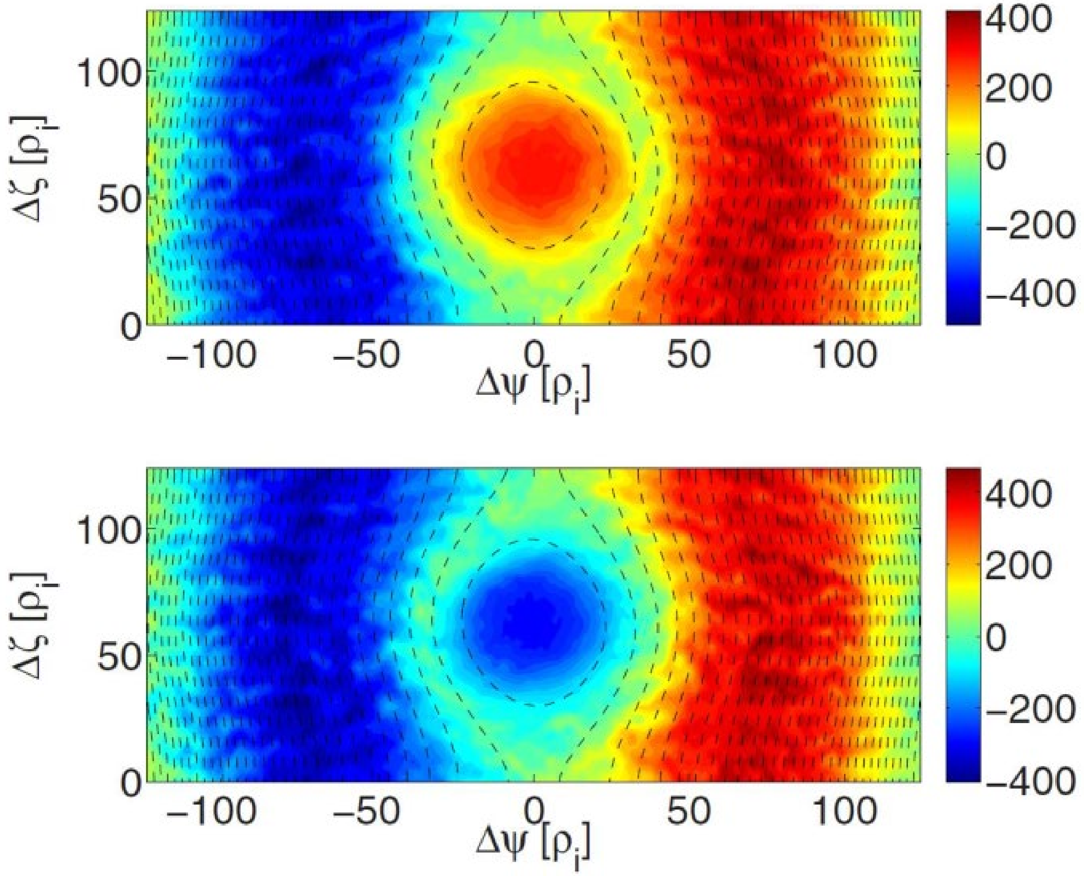

Hornsby et al. 2010;

- The presence of the island embedded in the turbulence not only generates flows around the island structure but also large scale electrostatic potential structures within the island which fluctuate in amplitude and sign. (votex mode, will promote the formation of E×B flow)

SUSTech Southern University of Science and Technology

Experiments--threshold

M. Jiang, Nucl. Fusion 59 066019 (2019)

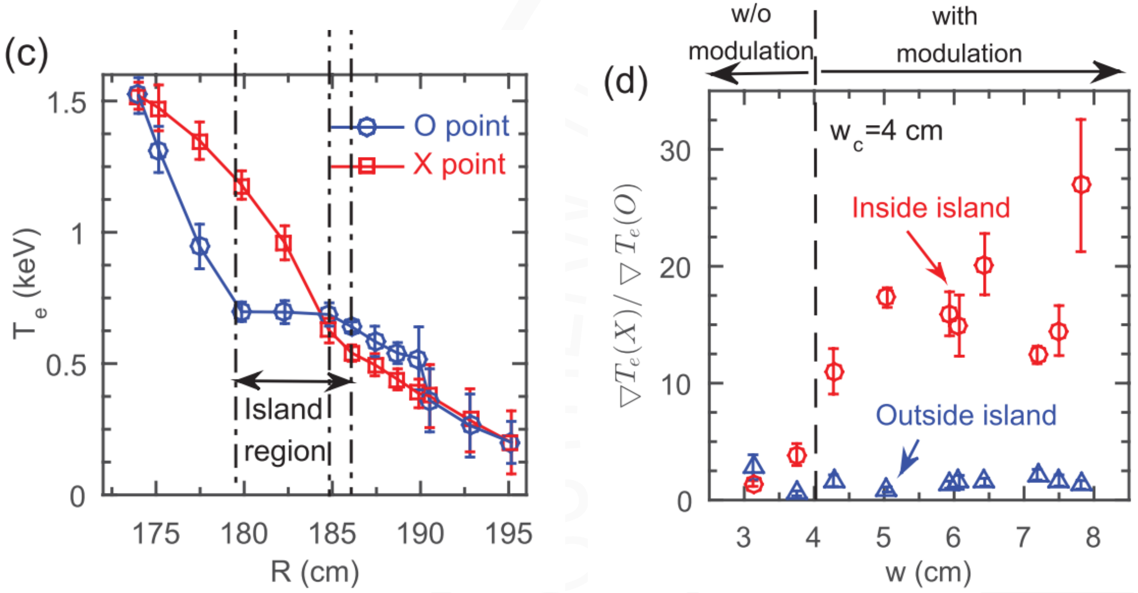

DIII-D (L. Bardóczi 2017 PoP)

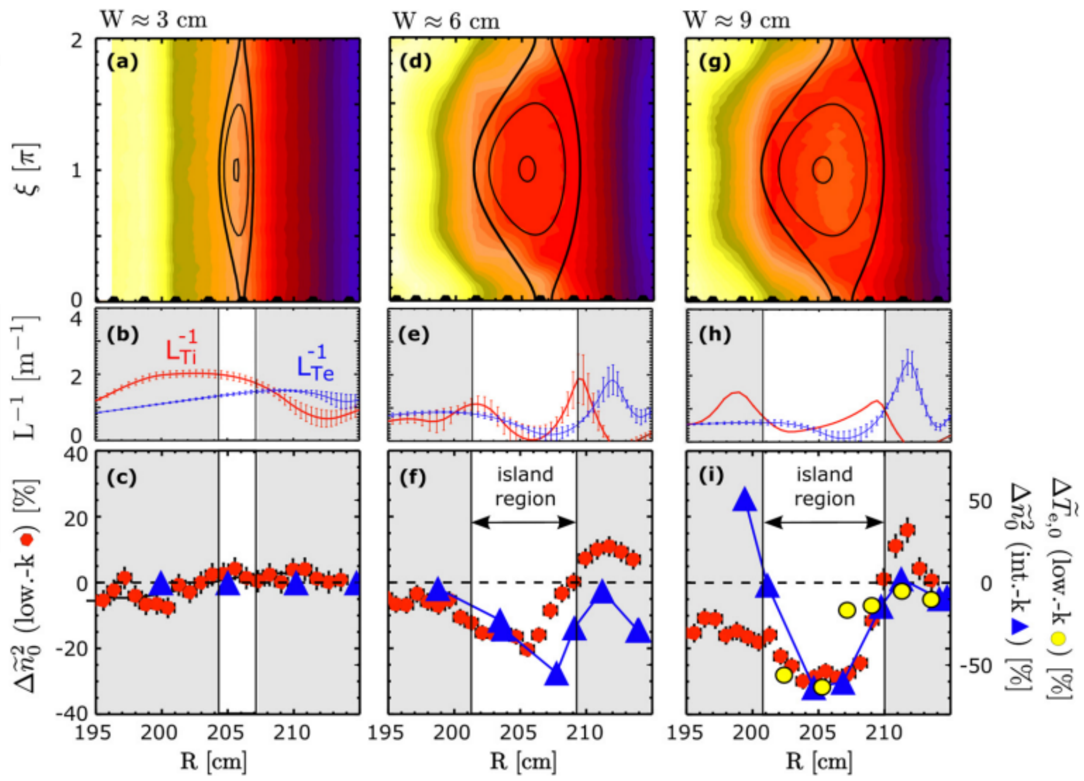

- It is the first evidence show that the turbulence modulation occurs only when the island width exceeds a certain threshold value $w_c \approx 10\rho_i \approx 4$ cm (with Fitzpatrick's analytical formula);
- All the low- and intermediate-k density and low-k temperature fluctuation strength are **reduced** inside a large island (W > 5 cm) where the local temperature gradient decreased.

(Note that the bottom row shows the % change of rotation averaged value relative to before NTM onset)

Experiments--2D plasma turbulence

Choi M.J. et al 2021
Nature Comm. 12 375

- The first evidence of localized modulation of large-scale turbulent density fluctuations by neoclassical tearing mode (NTM) has been reported in DIII-D tokamak[Bardóczi L. et al 2016 Phys. Rev. Lett.];

- Multi-scale interaction between MIs and microturbulence has been demonstrated through simultaneous two-dimensional measurements of the turbulence and the temperature and poloidal flow profiles in KSTAR tokamak.

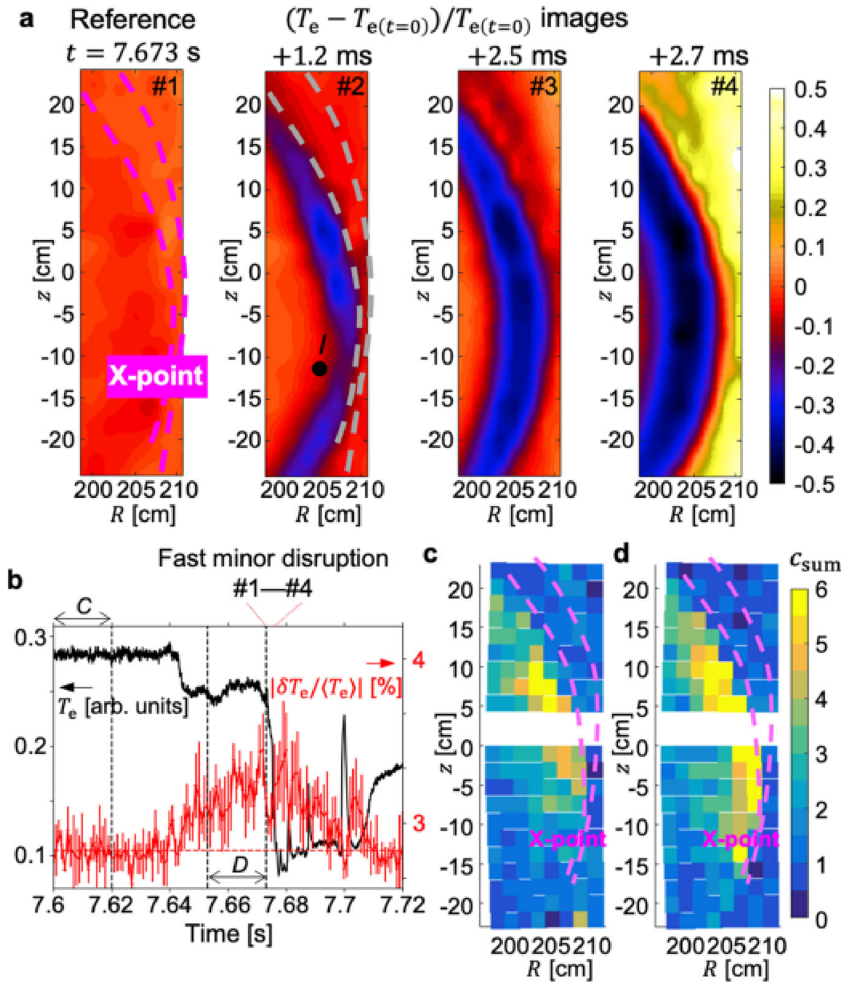

Turbulence enhancement at the reconnection site.

Spectral techniques

- The analysis methods used to characterize the statistical spectral feature of turbulence and the nonlinear coupling among MIs, GAMs and turbulence are mainly the **bispectrum** and **two-point correlation** techniques:

- The squared bicoherence for fluctuating parameters x(t), y(t) and z(t) with Fourier transforms X(f), Y(f) and Z(f) is defined by

$$\hat{b}^2_{XYZ}(f_1,f_2)=\frac{\left|\hat{B}_{XYZ}(f_1,f_2)\right|^2}{\left\langle\left|X(f_1)Y(f_2)\right|^2\right\rangle\left\langle\left|Z(f_3=f_1+f_2)\right|^2\right\rangle}$$

- The **two-point correlation technique** can provide a wealth of quantitative information about the structure of the turbulence and zonal flows, including the wavenumber (k) spectrum, the statistical dispersion relation and the turbulent broadening.

$$S(k,f)=\frac{1}{M}\sum_{j=1}^{M}I_{\Delta k}[k-k^j(f)]\left|S_1^j(f)+S_2^j(f)\right|/2$$

- This local wavenumber-frequency spectrum can be used to estimate the wavenumber spectrum width as follows

$$\bar{\sigma}_k^2(f)=\frac{\int[k-\bar{k}(f)]^2S(k,f)dk}{\int S(k,f)dk}$$

- The values of the correlation length (L_c) are estimated as the inverse of the k spectrum broadening, i.e., $L_c=1/\int\bar{\sigma}_k^2 df$

Gyrokinetic equations

The Gyro-kinetic equation in non-uniform magnetic plasma：

$$\frac{d}{dt} f_\alpha\left(\mathbf{R},\mu,v_\parallel,t\right)=\left(\frac{\partial}{\partial t}+\dot{\mathbf{R}}\cdot\nabla+\dot{v}_\parallel\frac{\partial}{\partial v_\parallel}\right)f_\alpha=0$$

$$\dot{\mathbf{R}}=v_\parallel\frac{\mathbf{B}}{B_0}+\frac{c\mathbf{b}_0\times\nabla\phi}{B_0}+\frac{v_\parallel^2}{\Omega_\alpha}\nabla\times\mathbf{b}_0+\frac{\mu}{m_\alpha\Omega_\alpha}\mathbf{b}_0\times\nabla B_0$$

$$\dot{v}_\parallel=-\frac{1}{m_\alpha}\frac{\mathbf{B}_0+\frac{B_0 v_\parallel}{\Omega}\nabla\times\mathbf{b}_0+\delta\mathbf{B}}{B_0}\cdot\left(\mu\nabla B_0+q_\alpha\nabla\phi\right)-\frac{q_\alpha}{m_\alpha c}\frac{\partial\delta A_\parallel}{\partial t}$$

$$\begin{aligned}\delta\mathbf{B}_{\mathrm{I}}&=\nabla\alpha\times\mathbf{B}_0\\&=\frac{\partial\alpha}{\partial\psi}I\nabla\psi\times\nabla\theta+\frac{\partial\alpha}{\partial\psi}g\nabla\psi\times\nabla\zeta\\&\quad+\left(\frac{\partial\alpha}{\partial\zeta}I-\frac{\partial\alpha}{\partial\theta}g\right)\nabla\zeta\times\nabla\theta.\end{aligned}$$

The island is introduced through a perturbed vector potential parallel to the background magnetic fleld

$$\mathbf{B}^*=\mathbf{B}_0^*+\delta\mathbf{B}_{\mathrm{I}}=\mathbf{B}_0+\frac{B_0 v_\parallel}{\Omega_i}\nabla\times\mathbf{b}_0+\delta\mathbf{B}_{\mathrm{I}}.$$

δf simulation method: weight equation $f=f_0+\delta f$

$$\frac{dw_i}{dt}=(1-w_i)\left[-\left(v_\parallel\frac{\delta\boldsymbol{B}}{B_0}+v_E\right)\cdot\frac{\nabla f_{0i}}{f_{0i}}+\left(\mu\frac{\delta\boldsymbol{B}}{B_0}\cdot\nabla B_0+q_i\frac{\boldsymbol{B}^*}{B_0}\cdot\nabla\phi+\frac{q_i}{c}\frac{\partial\delta A_\parallel}{\partial t}\right)\frac{1}{m_i}\frac{1}{f_i}\frac{\partial f_{0i}}{\partial v_\parallel}\right]$$

The HL-2A tokamak

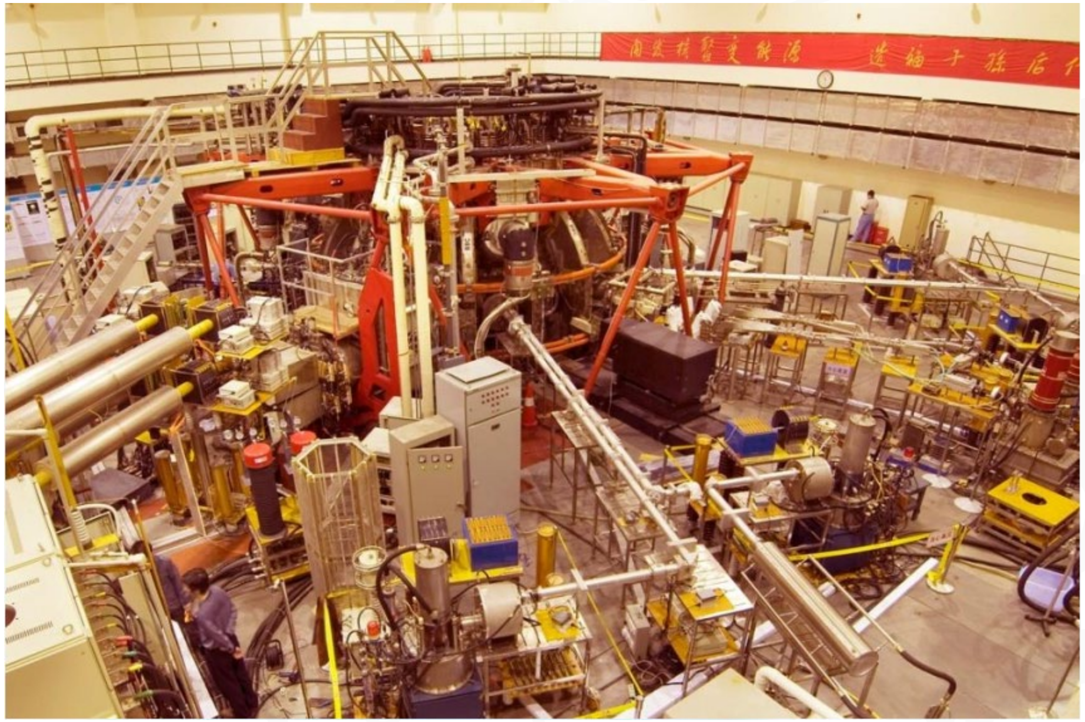

- R: 1.65 m
- a: 0.40 m
- B_t: 2.7 T
- I_p: 480 kA
- n_e: 6.0 x 10^{19} m^{-3}
- T_e: 5.0 keV
- T_i: 3.5 keV

- Completed in 2002, China's first larger tokamak device with magnetic divertor configuration.
- In 2009, the high confinement operation mode (H-mode) was realized for the first time, which is a milestone and significant progress in the history of magnetic confinement fusion experiments in China.

Auxiliary heating system:

- ECRH/ECCD: 5 MW
- NBI (co-injection) :4 MW
- LHCD: 2 MW (PAM, 3.7 GHz/2 s)

Experiment Results of Multiscale Interactions

SUSTech Southern University of Science and Technology

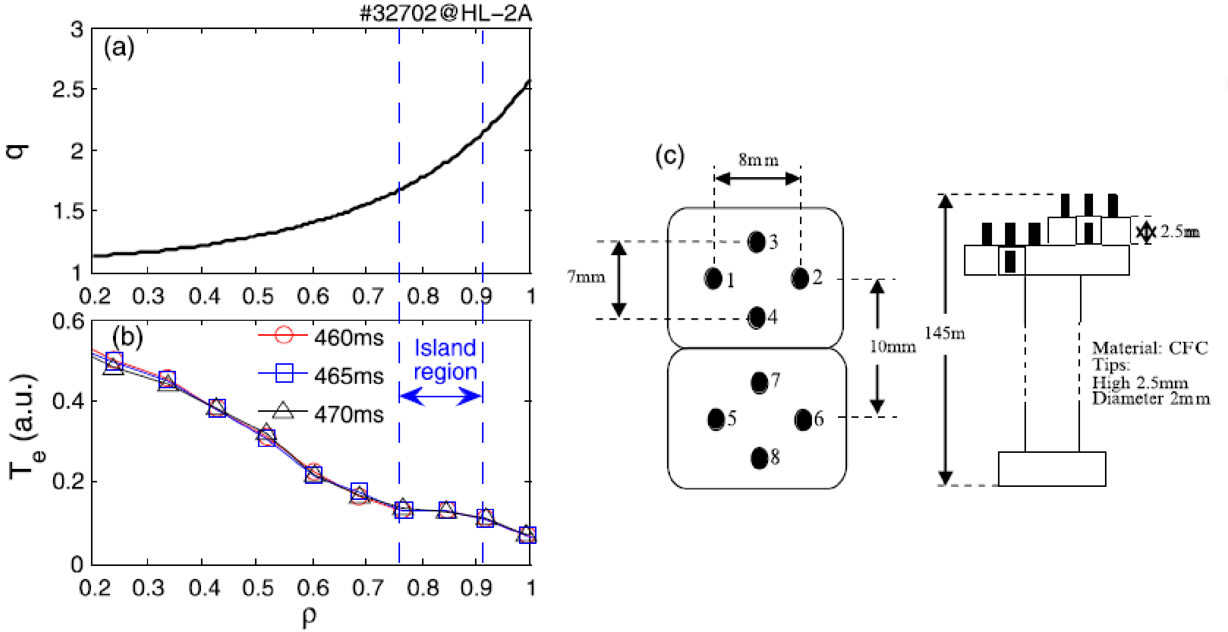

Fig.1 Magnetic island measured by ECE. (a) The safety factor q and (b) the T_e at different times with ρ

two step probe array and can detect the local n_e, t_e, E_r

- The T_e measured by electron cyclotron emission (ECE) system. The MI mainly exists in the region of about ρ=r/a=0.76-0.9, which is identified to be an (m/n)=(2/1) tearing mode.
- The position of the Langmuir probes is located at around 0.92.

Experiment Results of Multiscale Interactions

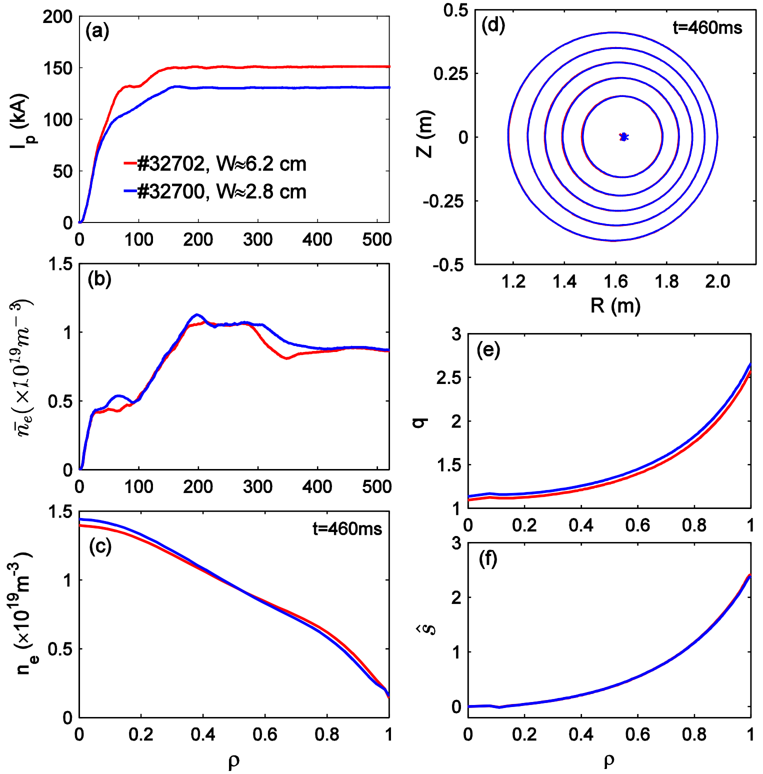

Fig. 2 Typical discharge waveforms of (a) plasma current, (b) line-averaged density. (c) electron density profile,

(d) flux surface shape, (e) safety factor profile and (f) magnetic shear for magnetic island widths of W≈6.2 cm (red) and W≈2.8 cm (blue).

- The electron density profiles and the magnetic flux surfaces have rather small difference for the two discharges.
- The lower plasma current leads to the higher safety factor, lead to different island width.
- GTC code have shown that the TMs are unstable in both cases whose growth rates are around γ=0.052 for shot 32702 and γ=0.043 for shot 32700, respectively.

Experiment Results of Multiscale Interactions

Southern University
of Science and

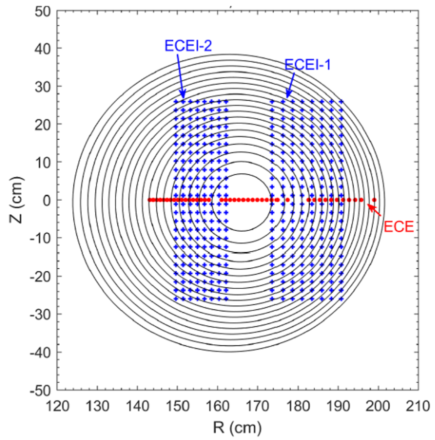

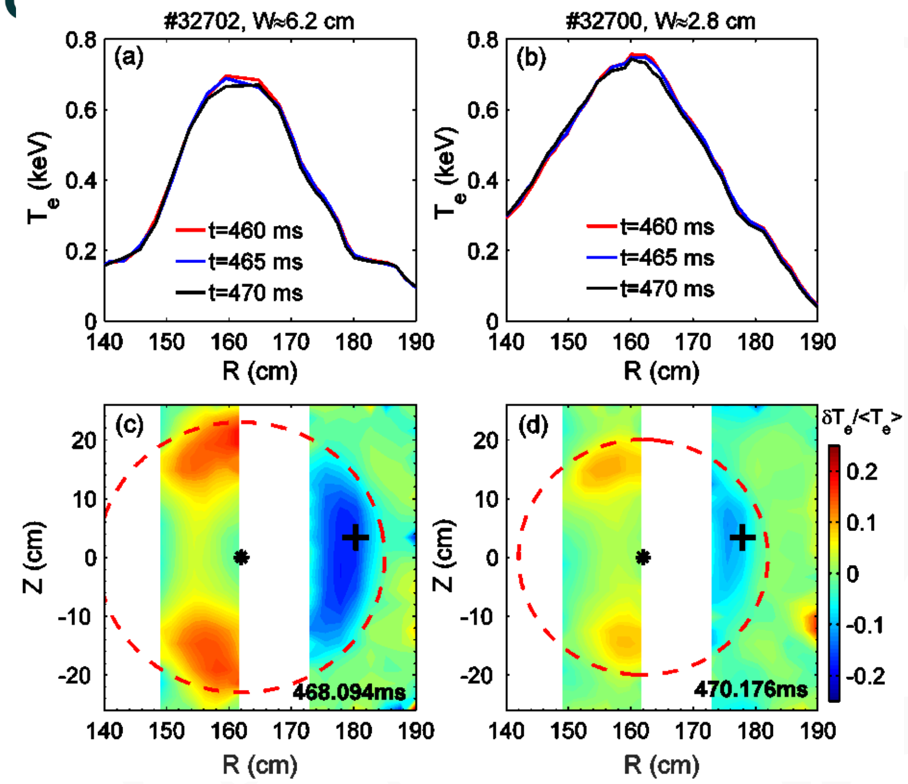

Fig. 3 (a,b)The corresponding electron temperature (Te) profiles;
(c,d)mode structures measured by electron cyclotron emission (ECE) and the ECE imaging (ECEI).

Different time, to show the process is stable, or MI and the turbulence are steady state.

J. Xu, J.C. Li et al Nucl. Fusion 2022

- It is identified that the MIs are resulted from (m/n)=(2/1) classical tearing modes and the widths can be evaluated by either the flattened regions of the T_e profiles or the correlation lengths of the mode structures in Figs. 3(c)-(d);

Experiment Results of Multiscale Interactions

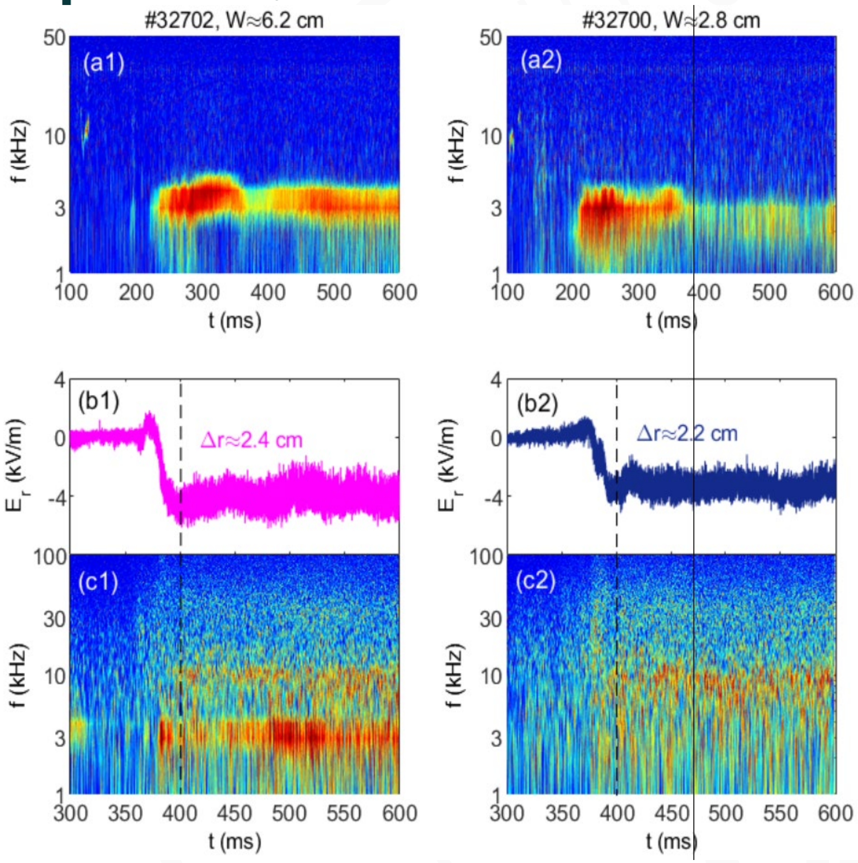

Fig. 4 (a) Spectrogram of SXR signal, time evolution of radial electric field and its spectrum for two values of magnetic island widths(b,c). (a1)-(c1) are the case for W≈6.2 cm while (a2)-(c2) are that for W≈2.8 cm, respectively.

- The MIs with frequencies about ~3.2 kHz are observed in both cases on the SXR signals and the amplitude in the case of large island(W≈6.2 cm) is significantly larger than that of small island(W≈2.8 cm);
- The mode at ~3.2 kHz is resulted from TM while the modes centered at ~9.4 kHz and 9.2 kHz are identified to be GAMs.

- The probes are inserted into the edge plasma whose radial positions with respect to the LCFS during the steady state are around ~2.4 cm and ~2.2 cm, corresponding to normalized radius of ρ=r/a≈0.93 and 0.94, respectively.

Experiment Results of Multiscale Interactions

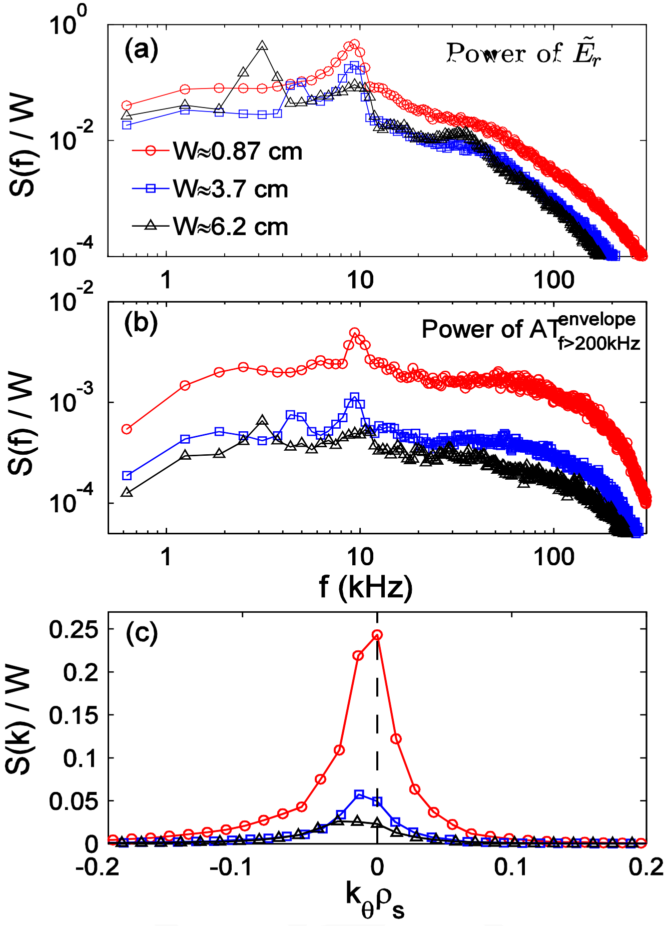

Fig. 5 Power spectrums of (a) electric field fluctuation Ẽr, (b) envelope of density fluctuation ñe with f >200 kHz and (c) normalized poloidal wavenumber for three different island widths.

- Both the amplitudes of Ẽr and envelope of high frequency turbulence are reduced at GAM frequency while they are increased at the MI frequency as the island becomes larger.

- The results also suggest that the MIs have strong impact on the background turbulence and they would decrease the coupling between GAMs and turbulence because the role of GAM in regulating the turbulence is partially taken over by the MIs.

Experiment Results of Multiscale Interactions

Southern University of Science and Technology

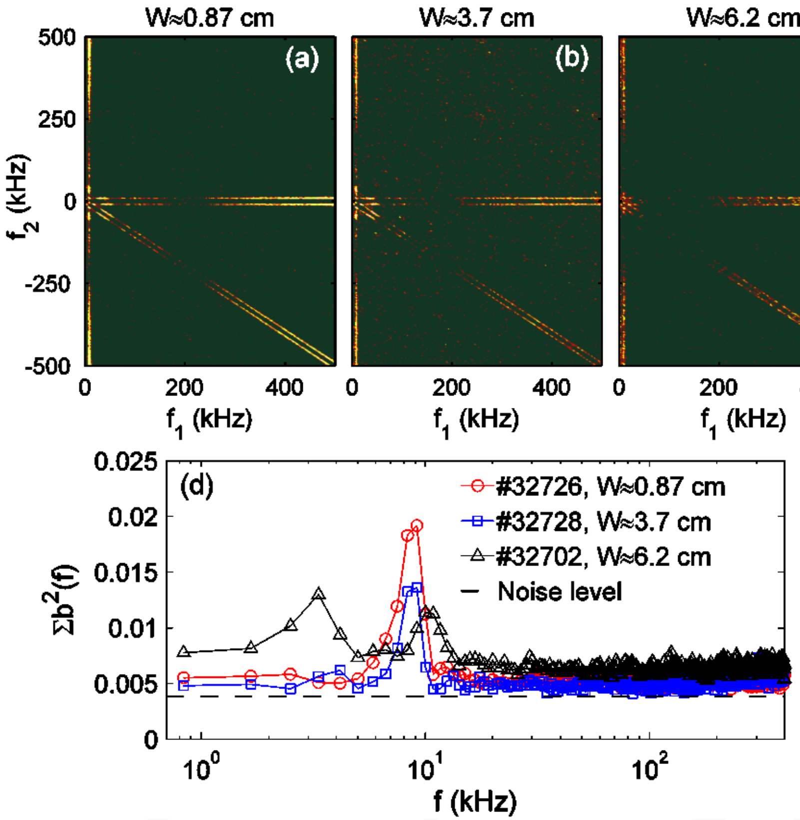

Fig. 6 Contour plots of autobicoherence of Ẽr for the case of (a) W≈0.87 cm, (b) W≈3.7 cm and (c) W≈6.2 cm. (d) the corresponding summed squared bicoherence.

- The strength of the nonlinear coupling between GAM and turbulence is decreased while it is increased between MI and turbulence as the island becomes larger, as indicated in Fig. 6(b) and Fig. 6(c) for W≈3.7 cm and W≈6.2 cm;
- In Fig. 6(d), it is clearly shown that the nonlinear coupling between GAM and turbulence becomes weaker while the nonlinear interactions between MIs and turbulence becomes stronger simultaneously with the increasing of the island size.

Experiment Results of Multiscale Interactions

SUSTech Southern University of Science and Technology

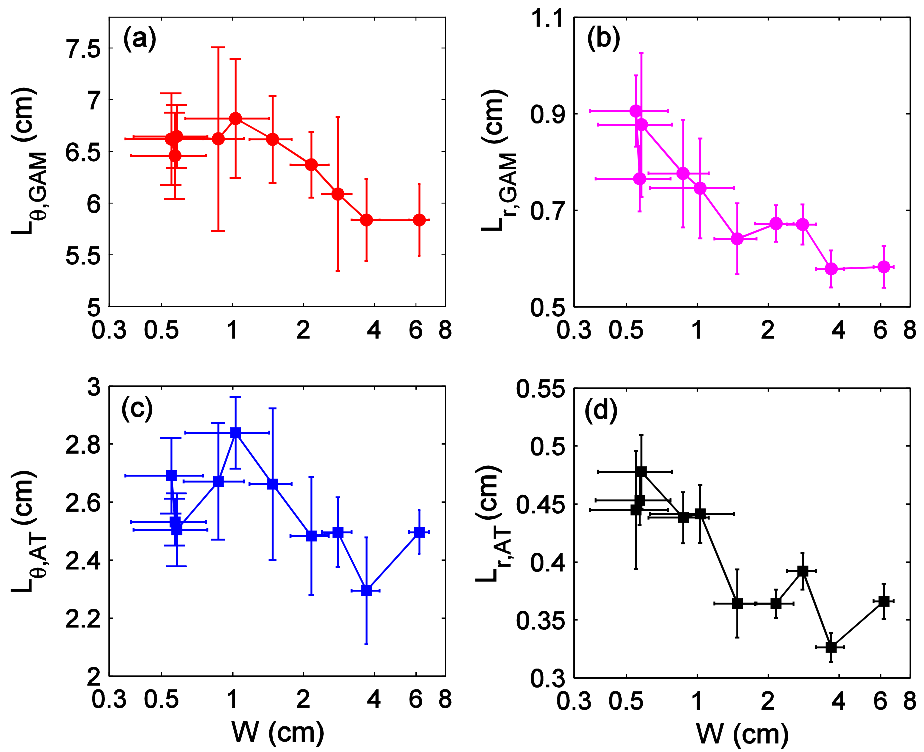

Fig. 7 Poloidal and radial correlation lengths of GAMs and turbulence as a function of magnetic island width.
(a) and (b) are the relationships for GAMs
(c) and (d) are those for turbulence, respectively.

- Both the poloidal and radial correlation lengths of GAM $L_{\theta,GAM}$ and $L_{r,GAM}$ show a gradual reduction when W ranges from 0.87 to 3.7 cm;
- The poloidal and radial correlation lengths of turbulence have nonmonotonic relationships with W, which show minimum at ~3.7 cm, implying that the magnetic islands around this width have relatively strong suppression effect on turbulent transport.

Numerical Results of Multi-scale Interactions

J.C. Li, J. Xu, Z. Lin 2022

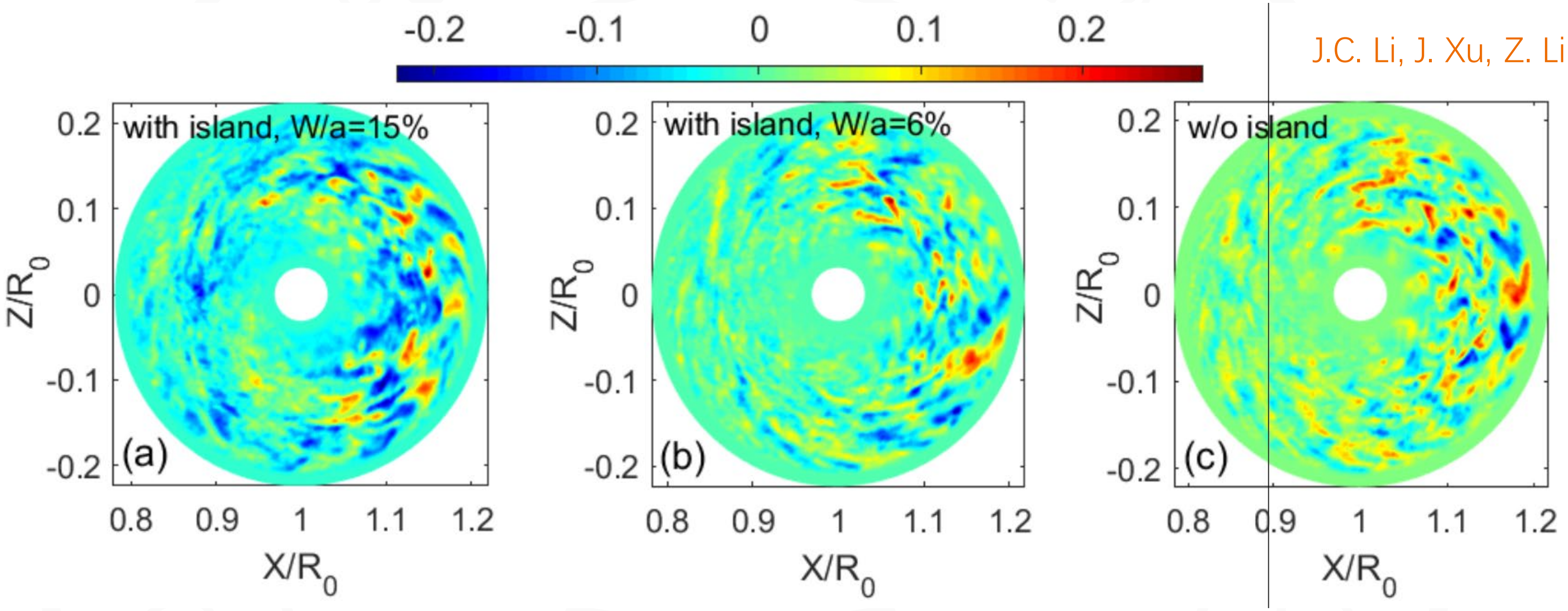

- The mode structure is much more chaotic when the magnetic island is implemented and the radial correlation length becomes smaller; while when the magnetic island is absent the radial flow structure is more obvious and the correlation length is larger ;
- The magnetic island can indeed suppress the drift-wave instabilities, leading to a decrease in the overall transport coefficient which is consistent with the results in Fig. 7(d).

Numerical Results of Multiscale Interactions

SUSTech Southern University of Science and Technology

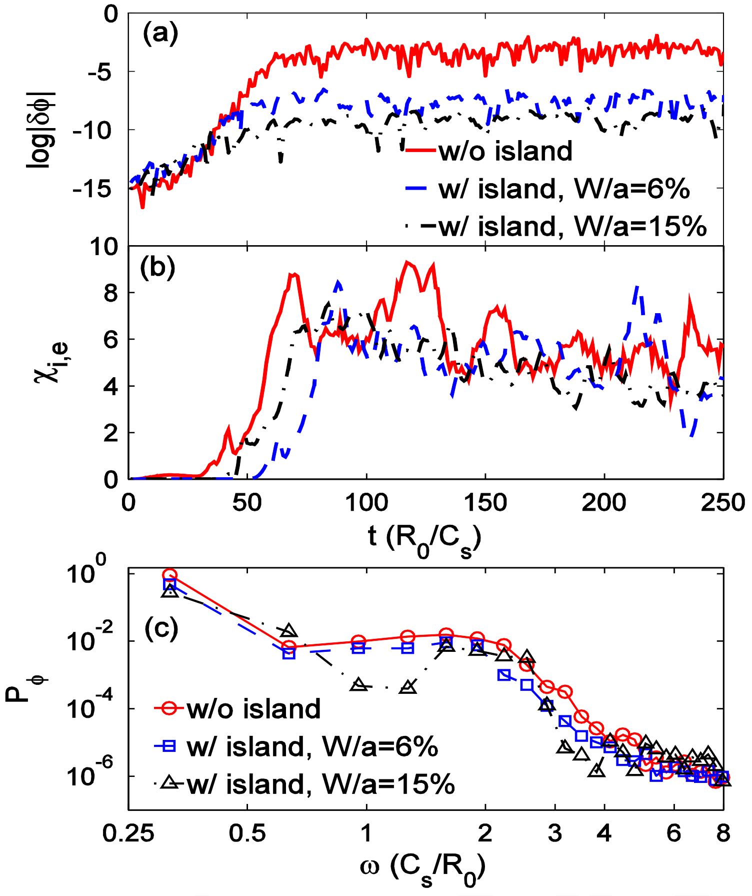

Fig. 9 Time evolution of (a) the magnitude of turbulence, (b) ion (electron) conductivity and (c) power spectrum of electrostatic potential during steady state for the cases of without MI (red), W/a=6% (blue) and W/a=15% (black).

- The turbulence transport (t =80-260 R_0/C_s) has a reduction of 9.4% and 15.8% with MI(W/a =6% and 15%) in comparison with the case of without MI, respectively;
- The radial correlation lengths of turbulence results in a decrease of 10.6% and 16.5% for the cases of W≈2.8 cm and W≈6.2 cm compared with that of W≈0.87 cm.
- The frequency spectrum of the potential shows a decrease in the amplitudes of both LFZFs and GAMs at 0.3 C_s/R_0 and 1.5 C_s/R_0(corresponding to a ~11.5 kHz, is extremely close to the experimental frequency of GAMs.

Numerical Results of Multiscale Interactions

SUSTech Southern University of Science and Technology

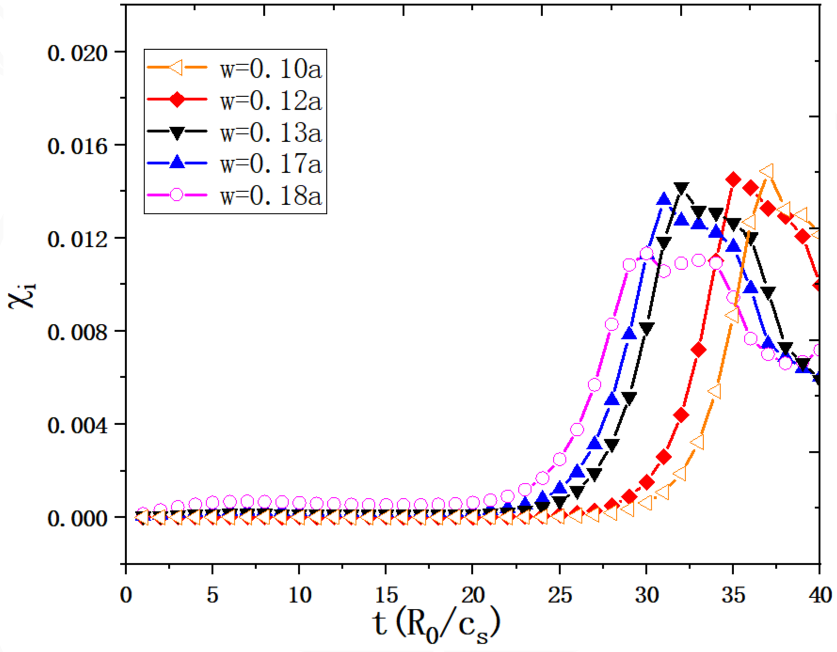

- The turbulence transport has a reduction with the increment of MI width;
- When the width of the magnetic island is less than about 0.1a (about 0.09a), the conductivity curve no longer increases.
- The turbulence transport also has a **nonmonotonic** relationship with the MI size, the turbulence transport does not increase continuously with the decrease of the magnetic island, the threshold island width is ~9%a.

CONCLUSION

- Statistical spectral features of the dependence of GAMs and their nonlinear couplings with AT on the MI width (W) in the edge region of HL-2A tokamak plasmas are analyzed；

- Experimental observations have indicated that the modulation influence as well as the strength of nonlinear interactions between GAMs and turbulence generally shows a **gradual decay** while the couplings between MIs and the latter are **increased** simultaneously **as the MI becomes larger**；

- By implementing a static MI, the gyrokinetic simulation demonstrates that the MI can indeed suppress the drift-wave instabilities, leading to a **decrease** in the overall transport coefficient which is consistent with the experimental results;

- Both experimental and numerical results show a nonmonotonic relationship between the lengths of turbulence and island width.

Some other works

TM and NTM with GTC code

- J. C. Li, et al **Phys. Plasmas**, 27:4, 042507(2020).
- J. C. Li, et al. **Phys. Plasmas**, 24, 082508 (2017)
- Y. Yao et al., **Physics Letters A**, 417, 127681(2021)
- J. C. Li, et al, **Phys. Plasmas** 26, 032505 (2019).
- Jizong Yang, Jingchun Li*, et al **AIP Advances** 10, 075005 (2020).

Drift wave and microturbulence

- J. C. Li, Z. Lin et al., **Plasma Phys. Control. Fusion**, 63, 125005 (2021).
- J. C. Li et al., **Plasma Sci. Technol.**, 22, 055101(2020)
- J.Q. Xu et al **Nucl. Fusion** 62 086048 (2022)

RFPs:

- J. C. Li, et al **Physical Review E** (2022, accepted)
- M. Jia*, J. C. Li* et al., **Nucl. Fusion**, 61, 046033(2021)
- J. C. Li et al., **Europhysics letters**, 127, 45002(2019)

Wave heating and current drive

- J. C. Li et al., **Plasma Phys. Control. Fusion,** 62, 095013(2020)
- J. C. Li et al., **Physics of Plasmas**, 22, 062512 (2015)
- J. C. Li et al., **Physics of Plasmas**, 22, 102510 (2015)
- J. C. Li et al., **Physics of Plasmas**, 23, 122504 (2016)

Thank you very much for your attention!